Published in final edited form as:
Magn Reson Med. 2014 October ; 72(4): 941–948. doi:10.1002/mrm.25009.

The Impact of Frequency Drift on GABA-Edited MR Spectroscopy

Ashley D Harris[1,2], **Benjamin Glaubitz**[3], **Jamie Near**[4], **C John Evans**[5], **Nicolaas A J Puts**[1,2], **Tobias Schmidt-Wilcke**[3], **Martin Tegenthoff**[3], **Peter B Barker**[1,2], and **Richard A E Edden**[1,2]

[1]Russell H. Morgan Department of Radiology and Radiological Science, The Johns Hopkins University, Baltimore, MD, USA.

[2]F. M. Kirby Center for Functional Brain Imaging, Kennedy Krieger Institute, Baltimore, MD. USA

[3]Department of Neurology, BG-Klinikum Bergmannsheil, Ruhr - University, Bochum, Germany.

[4]Douglas Mental Health University Institute and Department of Psychiatry, McGill University, Montreal, PQ, Canada.

[5]CUBRIC, School of Psychology, Cardiff University, Cardiff, UK.

Abstract

Purpose—To investigate the quantitative impact of frequency drift on GABA+-edited MRS of the human brain at 3T.

Methods—Three sequential GABA+-edited MEGA-PRESS acquisitions were acquired in fifteen sessions; in ten of these, MRS was preceded by fMRI to induce frequency drift, which was estimated from the creatine resonance at 3.0 ppm. Simulations were performed to examine the effects of frequency drift on the editing efficiency of GABA and co-edited macromolecules (MM) and of subtraction artifacts on GABA+ quantification. The efficacy of post-processing frequency correction was also investigated.

Results—Gradient-induced frequency drifts affect GABA+ quantification for at least 30 minutes after imaging. Average frequency drift was low in control sessions and as high as -2 Hz/min after fMRI. Uncorrected frequency drift has an approximately linear effect on GABA+ measurements with a -10 Hz drift resulting in a 16% decrease in GABA+, primarily due to subtraction artifacts.

Conclusion—Imaging acquisitions with high gradient duty cycles can impact subsequent GABA + measurements. Post-processing can address subtraction artifacts, but not changes in editing efficiency or GABA:MM signal ratios, therefore protocol design should avoid intensive gradient sequences prior to edited MRS.

Keywords

Edited MRS; GABA; frequency drift; subtraction artifact; editing efficiency

Corresponding Author: Richard Edden, Division of Neuroradiology, Park 367C, The Johns Hopkins University, School of Medicine, 600 N Wolfe Street, Baltimore, MD, 21287, Phone: +1-410-614-3418, fax: +1-410-502-6076.

Introduction

Edited MR spectroscopy (MRS) is being increasingly used to quantify metabolites that have previously been difficult to resolve in the *in vivo* spectrum. γ-aminobutyric acid (GABA), the primary inhibitory neurotransmitter, is widely measured using edited MRS (1,2) in studies of healthy brain function (combining of GABA measurements with behavioral tasks (3–6) and functional neuroimaging (7–12)) and a range of clinical conditions (13–19).

Edited MRS separates signals of interest from other overlying signals by exploiting known couplings. In the case of GABA, a frequency-selective pulse can be applied to GABA spins at 1.9 ppm to modify the evolution of GABA spins at 3.01 ppm. Two subspectra are acquired, one with the 1.9 ppm editing pulse ("ON") and one without the editing pulse ("OFF"). The difference between these subspectra contains a GABA signal at 3.01 ppm, while overlying signals (in particular from creatine (Cr)) are removed (as in Figure 1a). While this method is conceptually simple, accurate subtraction of the larger Cr signal is required (20,21). One major limitation of this method is that insufficiently selective editing pulses results in co-editing of macromolecular (MM) signal at 3 ppm (due to a coupling to a signal at 1.7 ppm that is partially inverted by the editing pulses) as well as other metabolite species such as homocarnosine; the edited GABA signal is therefore widely referred to as GABA+. One source of error is B_0 field drift during the experiment. This has two effects on edited spectra: (1) subtraction artifacts resulting from misalignment of the Cr signal in the ON-OFF subspectra (Figure 1b) and (2) changes in editing efficiency of GABA and MM as the frequency of the editing target resonance drifts relative to the constant frequency at which the editing pulse is applied (Figure 1c).

The B_0 field is generally extremely stable. However, the application of field gradients during scanning deposits power, heating various scanner components, in particular the passive shim elements (22–24). This heating, and associated cooling, results in changes in the B_0 field. These "gradient-induced field drifts" are problematic for MRS studies (25), and may persist for hours (22,24,25). The level of gradient-induced field drift depends the quantity and placement of ferrous shim elements in an individual scanner (24,25) and the gradient duty-cycle causing the power deposition. While passive shim elements are limited in some modern systems, there may be multiple factors that contribute to gradient-induced field drifts (22). The combination of MRS with other imaging, such as diffusion and functional MRI (fMRI), makes characterizing, understanding and correcting these frequency drifts important.

Post-processing correction methods to address frequency instability in GABA+-edited MRS have been proposed elsewhere (20,21,26), but often without differentiating between instabilities due to field drift or subject motion. Improved linewidths and/or SNR can be achieved in non-edited MRS by applying frequency correction either prospectively or retrospectively (23,25,27–29). Difference-edited MRS requires substantially greater stability since frequency instability may introduce subtraction and other artifacts (1,2,20,21,26).

The purpose of this manuscript is to quantify the field drifts caused by a single typical fMRI scan, to determine whether drifts of this size can impact subsequent GABA+ quantification,

to investigate potential mechanisms causing this effect, and to evaluate a post-processing field-drift correction scheme. This was accomplished by acquiring repeated *in vivo* GABA+-edited MRS data, both under stable conditions as well as following an 8-minute fMRI acquisition, and by performing simulations to investigate the independent impact of frequency drift on subtraction artifacts and editing efficiency of GABA and the co-edited MM signal.

Methods

Data were acquired at 3T. The main experimental data were acquired with a 32-channel head coil Philips Achieva system. Supplemental data were collected on a GE HDx system. The local Institution Review Boards (Johns Hopkins University School of Medicine, the ethics committee of the Ruhr – University Bochum and the ethics committee of the School of Psychology, Cardiff University) approved study protocols and all participants provided written informed consent.

Frequency Drift Quantification

Three sequential edited MRS acquisitions were performed in each of 15 sessions. For 10 of these sessions (5M/5F), an fMRI acquisition (TR/TE = 2500 ms/35 ms, 200 repetitions, field of view: 224 × 232 mm^2, 112 × 110 matrix, 39 3-mm slices, SENSE acceleration factor of 3, scan duration 8.3 minutes, maximum gradient amplitude = 80 mT m^{-1}, slew rate = 100 mT m^{-1} ms^{-1}) was performed prior to MRS to generate gradient-induced frequency drift. This is intended as a “standard” fMRI scan, using default parameters for detecting BOLD activation. The remaining 5 “control” studies (2M/3F) were without fMRI (see Figure 2b for the protocol). Four subjects participated in both sessions (average age of 11 subjects: 27 ± 2.5 years). GABA+-edited MEGA-PRESS (30) was acquired using 14-ms sinc-Gaussian editing pulses (full-width half-maximum inversion bandwidth 86.6 Hz) applied at 1.9 ppm (ON scans) and 7.46 ppm (OFF scans). The 3×3×3 cm^3 voxel was located in the precuneus (as seen in Figure 1a). Other scanning parameters included: TR/TE = 2s/68 ms; 320 transients acquired in 20 dynamic scans, each composed of a 16-scan phase cycle, with editing pulse frequency (OFF/ON) alternating with each dynamic scan; 2048 data points sampled at a spectral width of 2 kHz, VAPOR water suppression. We use the term “a dynamic” to mean one phase cycle, for example 16 scans that are acquired in a consecutive block with the same editing frequency; editing frequency is updated with alternating dynamics. In PRESS experiments, phase-cycling is used to eliminate residual magnetization from outside the voxel that is not already suppressed by the crusher gradients. All time-domain datasets were zero-filled by a factor of 16 and 3 Hz exponential line broadening was applied. The frequency drift during each acquisition was quantified by the Cr peak fit with a Lorentzian model using Gannet (31). Quantitative analysis was also performed in Gannet, modeling the GABA+ peak in a single fit, using a five parameter Gaussian model; Gaussian height, width and frequency with a baseline offset and linear slope determined within the spectrum from 2.75–3.55 ppm. The water signal was modeled as a Gaussian-Lorentzian function. The ratio of the integrals of the modeled GABA+ and water peaks, making corrections for water content, T1, T2 and editing efficiency, were used to quantify GABA+ in institutional units (i.u.) (2) using

$$[\mathrm{GABA}]=\frac{S_{\mathrm{GABA}}}{S_{\mathrm{H2O}}}[\mathrm{H_2O}](\mathrm{vis}_{\mathrm{H2O}})\frac{1-\exp\left(\frac{-\mathrm{TR}}{\mathrm{T}_{1\mathrm{H_2O}}}\right)}{1-\exp\left(\frac{-\mathrm{TR}}{\mathrm{T}_{1\mathrm{GABA}}}\right)}\times\frac{\exp\left(\frac{-\mathrm{TE}}{\mathrm{T}_{2\mathrm{H_2O}}}\right)}{\exp\left(\frac{-\mathrm{TE}}{\mathrm{T}_{2\mathrm{GABA}}}\right)}\times\frac{\mathrm{MM}}{\kappa} \quad \text{Eq. 1}$$

S_{GABA} and S_{H2O} are the integrals of the modeled GABA+ and water peaks, respectively. Pure water concentration, $[H_2O]$ = 55,000 mmol/dm^3, water visibility (vis_{H2O}) = 0.65 (32,33), the T1 and T2 used for water are 1.1s and 0.095s, respectively (34), and the T1 and T2 of GABA are 0.80s (intermediate between MM (35) and GABA (36)) and 0.088s (37), respectively. MM is approximated by the constant 0.45 (2) to account for the MM content; this constant does not address changes in MM fraction arising from drift, regional and individual differences etc. κ is the editing efficiency and is assumed to be 0.5 (2).

The relationship between frequency drift and GABA+ was quantified using a linear fit including datapoints that had a negative frequency drift (less than 1.5 Hz positive drift) across the acquisition. A repeated-measures ANOVA was used to examine the effects of time (MRS scans 1–3) and group (control/fMRI) on quantified GABA+ concentration.

Editing Efficiency Simulations

Changes in GABA and MM as a function of frequency drift were first examined by simulating the offset-dependence of the editing efficiency, and secondly by averaging across offsets to investigate the drift dependence. The 3.0 ppm GABA peak and the co-edited MM peak were independently simulated for editing pulse offsets from 0 Hz to −80 Hz in increments of 1.25 Hz (*i.e.* simulating the editing pulse applied at 1.9 to 1.275 ppm). Simulations were performed as described previously (38), whereby the density matrix formalism was used to generate simulated MRS data, using ideal instantaneous excitation and refocusing pulses. Simulations were performed for the GABA spin system (38) at a simulated field of 3T with 14 ms sinc-Gaussian editing pulses (as used in experiments). Prior Bloch equation simulations of the shaped editing pulses were used to determine the flip angle experienced by each of the GABA spins; editing pulses were incorporated into the MEGA-PRESS simulation as instantaneous rotations of these calculated flip angles. To account for the fact that the intensity of the 1.9 ppm GABA peak is spoiled in the ON-experiments, the excitation pulse was not applied to those spins in the ON-experiments. Similarly, the effects of signal offset on the MM signal contribution was investigated using the same formalism but using a 1.7 ppm resonance for MM to replace the 1.9 ppm GABA resonance (35). Frequency drift impact on editing efficiency for both GABA and MM across an experiment were simulated by averaging 64 ON-OFF pairs where the first pair had 0 Hz editing pulse offset and the last was shifted by a total drift of 0, -4, -8, -12, -16 and -20 Hz, with linear interpolation of editing offset for the intermediate dynamics. As the MM signal contribution to GABA+ (39,40) is likely to vary between sequences and brain regions, a range of relative signal contributions (40–60%) were examined.

Subtraction Artifact Simulations

Creatine subtraction artifacts overlap with the edited GABA+ signal and potentially interfere with GABA+ quantification. These artifacts were simulated (independent from editing

efficiency effects) by artificially adding a frequency shift to an *in vivo* dataset. This *in vivo* data set (TR/TE = 2 s/68 ms; 320 transients acquired in 40 dynamic scans of 8 phase-cycles; 14 ms editing pulses applied at 1.9 ppm; 2048 data points; spectral width = 2 kHz) was acquired at the beginning of the day. The small frequency drift that occurred was removed by aligning the residual water peak (based on the complex maximum in each spectrum). Different magnitudes of linear frequency drift were applied to generate total frequency drifts of -5 Hz, -10 Hz, -15 Hz and -20 Hz across the dataset. GABA+ concentration was then quantified as described above.

First, the acquired data were reordered to mimic an acquisition protocol of 20 dynamic scans of 16 phase cycles, so this simulation would be directly comparable to the main *in vivo* experimental data. In a secondary analysis investigating the impact of the frequency of alternating between ON and OFF scans, (*i.e.*, the degree of interleaving), the same total simulated drifts were applied to the original (*i.e.*, acquisition of 40 dynamics of 8-scan phase cycles) data to compare interleaving 8-scan blocks to 16-scan blocks.

Frequency Correction

Frequency correction (20) was applied to the main *in vivo* experimental data to evaluate its efficacy. Briefly, the Cr peak of each ON and OFF subspectra was modeled as a Lorentzian and realigned. The choline peak was used to correct differences between the ON and OFF subspectra. After this frequency correction, GABA+ concentration was quantified as described above and a paired t-test was applied to compare GABA+ concentration with and without frequency correction.

Results

Three consecutive GABA+-edited spectra were acquired in fourteen subjects. One (control) subject did not complete the third scan, but the first two scans were included.

Frequency drift quantification

When MRS is performed after fMRI, a substantial increase in frequency drift is observed and this frequency drift can persist for at least 30 min (as shown in Figure 2b). Frequency drift was quantified by a linear fit of frequency over time (as shown in Figure 2c). This linear fit represents the drift well, $R^2 = 0.85 \pm 0.25$ across all fits. The average frequency drift rates in first, second and third control scans were 0.025 ± 0.23 Hz/min, 0.074 ± 0.16 Hz/min and 0.098 ± 0.19 Hz/min, respectively, while after fMRI drift rates were −1.22 ± 0.32 Hz/min, −0.91 ± 0.26 Hz/min and −0.48 ± 0.18Hz/min. Student's t-tests confirm the drift rate is significantly different between fMRI and control sessions ($p < 0.001$ for each of the three comparisons). The repeated-measures ANOVA indicates that group (control/fMRI) has a significant effect on quantified GABA+ ($p < 0.05$).

Measured GABA+ concentration is plotted against the drift rate in Figure 2d. By visual inspection, one outlier was identified and was not considered in further analyses. Positive frequency drift is poorly defined because in practice it occurs infrequently, therefore datasets with a positive drift of 1.5 Hz or greater over the acquisition were excluded from further analyses (excluded points are represented with open circles). GABA+ measurement is

linearly correlated with frequency drift, ($R^2 = 0.27$, $p < 0.001$); for example, a -10 Hz frequency drift predicts a 16% decrease in GABA+.

Editing Efficiency

In Figure 3a, the 3 ppm GABA peak changes appearance as the editing pulse moves off-resonance, resulting in a reduced integral (as shown in Figure 3b). These simulations are consistent with the phantom data reproduced from (41). The GABA signal decreases and the co-edited MM signal initially increases as the editing pulse is offset (as shown in Figure 3b). Figure 3c shows the drift-dependence (rather than offset-dependence) of the editing efficiency for both MM and GABA. For a -10 Hz frequency drift, GABA signal loss on the order of a 1.5% whereas the co-edited MM signal shows a 10% increase. The net effect on GABA+MM signal depends on the relative contributions of GABA and MM to the GABA+ signal (as shown by the gray area in Figure 3c representing 40:60 to 60:40 relative contributions of GABA:MM). Assuming initially signal contributions of 50:50, a -10 Hz frequency drift will result in +4% GABA+ signal change and the relative contributions of GABA:MM will change to 47:53 as shown in Figure 3c. A 60% initial MM contribution would change to 63% after -10 Hz drift.

Subtraction Artifacts

Figure 4a shows the GABA+ peak reduces with drift due to imperfect subtraction of the Cr signal. The zero-drift spectrum appears approximately Gaussian, the intermediate spectra more triangular and the -20 Hz-drift spectrum appears to have “pseudo-doublet” character. The effects on quantified GABA+ concentration are shown in Figure 4b, a -10 Hz drift over an acquisition predicts an 11% reduction in GABA+ measurement.

The degree of interleaving ON-OFF cycles impacts the observed subtraction artifact. Doubling the rate of interleaving (while maintaining the same total number of transients) approximately halves the relative loss in measured GABA+ (a -10 Hz drift over the more interleaved acquisition predicts only in a 5.9% reduction in GABA). The 3 ppm GABA resonance is qualitatively similar in appearance, although consistent with greater subtraction artifacts at slower rates of interleaving.

Frequency Correction

Losses in the GABA+ measurement due to the subtraction artifact appear to be largely corrected after applying frequency correction. Post-correction datapoints (filled) are almost all higher than pre-correction (open) datapoints (as shown in Figure 5a). The correlation between GABA+ concentration and frequency drift was largely removed after frequency correction ($R^2 = 0.11$; Figure 5b). The linear fit of GABA+ concentration as a function of frequency drift, with the intercept constrained to match that in Figure 2e, was −0.0038 i.u./Hz. There is a significant increase in GABA+ concentration with frequency correction ($p<0.001$), with an average increase of 21±16% and the coefficient of variation reduces from 26% prior to correction to 18% with frequency correction.

Discussion

Frequency drift increases linewidth and measurement uncertainty in PRESS spectroscopy (25). Implementing post-processing frequency correction has been previously advocated for GABA+-edited MEGA-PRESS (21), and improves measurement repeatability (20). The quantitative impact of frequency drift and its subsequent correction on *in vivo* GABA+ measurements have not previously been shown.

Drifts of -10 Hz over a 10-minute acquisition were common and impacted GABA+ measurements. An 8-minute fMRI run can cause significant frequency drifts up to 30 minutes later (as shown in Figure 2c). Interestingly, the control study and two fMRI studies with the largest negative drifts (Figure 2c and 2d) were performed after an MR exam that included multiple fMRI/diffusion imaging runs, providing evidence that frequency drift may persist between MR exams. In Supplementary data, we present drift examples from three other 3T scanners (two Philips Achieva, one GE Signa HDx). On both Philips scanners, the drift after an 8-min fMRI run is appreciable (as shown in Supplementary Figure a). By contrast, drift appears minimal after a 5-min fMRI run on the GE system (shown in Supplementary Figure b). Clearly, field drift differs between scanners, and this manuscript provides a template to quantify drift on individual systems. Drift will be influenced by gradient strength, system design (*i.e.*, the quantity of iron shim elements) and system stability. As inherent magnet homogeneity improves, fewer shim elements are required; nevertheless, passive shimming is used to extend the field-of-view. Superconducting shims used as an alternative to iron shims and are expected to reduce frequency drift. When comparing frequency drift between scanners both in this manuscript (refer to Supplemental Figure a) and in Ref (25), greater drift was observed in the system with more shim iron installed. MRS acquisitions are less gradient-intensive than imaging acquisitions, therefore cooling (negative frequency drift) is most relevant to mixed MRI/MRS protocols. The impact of positive frequency drift is not well sampled by this *in vivo* dataset because the gradient duty cycle during MRS was insufficient to cause substantial gradient heating. Therefore, only data showing frequency drifts of less than 1.5 Hz (zero-drift datasets included) over the scan were used to examine the relationship between frequency drift and GABA+ concentration.

Negative frequency drifts reduce the editing efficiency of GABA and increase the editing of MM (as the degree of inversion of the MM signal at 1.7 ppm increases). The MM signal fraction of GABA+ is at least 40% (39,40), but likely varies with sequence parameters (TR and editing pulse bandwidth), brain region and individual differences. As seen in Figure 3c, the total GABA+ signal changes modestly due to editing efficiency effects because the changes in GABA and MM have opposite sign. Although GABA+ changes due to editing efficiency effects are modest, it is important to recognize that the relative contributions of GABA and MM to the GABA+ signal changes with frequency drift. For example, assuming equal signal contributions of GABA and MM (50:50) at 0 Hz drift, the relative signal contributions will change to 47:53 with 10 Hz drift. This has implications for studies examining GABA differences between groups/conditions by making GABA+ measurements as changes in GABA:MM complicate the interpretation of data.

As long as the frequency drift is small compared to the bandwidth of the editing pulses, efficiency effects will remain relatively small. Within a 68 ms TE, editing pulse duration is generally limited to ~14 ms and the editing selectivity of GABA+-edited MRS is broadly similar (although some 3T scanners can achieve B_1 fields of approximately 20 uT, so permit more selective editing pulses of over 20 ms (42), since the slice-selective pulses are shorter). It is possible to suppress the MM contribution (39), by placing editing pulses in OFF and ON scans symmetrically about the MM resonance at 1.7 ppm (i.e. ON 1.9 ppm and OFF 1.5 ppm). This removes the confound of MM that is present in GABA+ experiments and would remove any overestimation of GABA+ due to MM; however, frequency drifts will interrupt the symmetry of this arrangement and result in a gradual return of MM contributions.

Subtraction artifact due to misalignment of the Cr spectra is the dominant source of GABA+ underestimation; a simulated -10 Hz drift results in an 11% signal loss, which is on the order of the total losses observed (16%). Other sources of signal loss may explain the discrepancy, such as order effects and subject compliance. The effect of frequency drift on signal localization is expected to be minimal as even a 20 Hz drift is minor compared to the ~1.4 kHz refocusing pulse bandwidth. This results in a linear shift in voxel location of the order of 1% of the voxel size, in each direction defined by a refocusing pulse. This shift is small and for most brain regions is unlikely to include new tissue with no GABA, so the impact on measurements will also be small. The residual water signal, which will gradually increase as drift worsens the water suppression, will also cause drift-dependent subtraction artifacts in edited spectra, as seen in Figure 1b. This may result in substantial disturbances to the baseline, and negatively impact quantification of GABA+ unless appropriate analysis methods are used to deal with such baseline distortions.

Crusher gradients are applied to dephase out-of-voxel signal contamination. However, due to TE limitations in the MEGA-PRESS experiment, the duration of these gradients is limited and therefore signal suppression by gradients is imperfect. Phase cycling augments voxel localization without additional averages and no impact on TE (2), but is usually implemented at the expense of rapid interleaving, resulting in proportional losses in measured GABA+ concentration. One possible improvement to the implementation used here is to allow phase cycling across editing interleaves.

The frequency correction scheme (20) used here generally increases GABA+ measurement (as shown in Figure 5) by correcting subtraction artifacts, resulting in GABA+ measurements closer to the expected no-drift condition. Although some consequences of gradient-induced frequency drift may be corrected, substantial variance remains; the coefficient of variation across all scans is reduced from 26% before frequency correction to 18% after, equivalent to a 19% removal of independent variance. The remaining variance may be due to imperfect frequency correction, the uncorrected consequences of editing efficiency, varying signal contributions of GABA and MM, and residual water artifacts. It is prudent to avoid drift errors where possible, for example by ordering imaging protocols such that MRS acquisitions occur prior to scans with high gradient duty cycles, by using MRS acquisitions with highly interleaved ON and OFF subspectra.

Prospective frequency correction aims to correct the drift at its source, removing both subtraction artifacts and editing efficiency changes, including changes in the GABA:MM signal contribution. A small flip-angle water navigator can be used to acquire an unsuppressed water signal as a metric for magnetic field instabilities, motion artifacts and severely corrupted transients (29). This method has been adapted to provide an index to reject motion-corrupted data from MEGA-PRESS GABA+ acquisitions (26). To mitigate drift for PRESS in real-time, the unsuppressed water signal can be used to update the RF carrier frequency (25), using online reconstruction and feedback of the water resonance frequency to update the carrier frequency of the RF pulses and the analog-to-digital converters. Further expansion of this method to MEGA-PRESS could minimize the need for post-hoc frequency correction. Similarly, on Philips systems a water-based field lock option exists and is reported to maintain the carrier frequency to within 2 Hz (21). It is important to stress that the general aim of frequency-lock methods is to reduce the linewidth of standard averaged spectra, and that the requirements for difference editing are substantially different. The timing and accuracy of the prospective frequency updates is crucial to avoid causing, rather than removing, subtraction errors (43). Data presented in Supplementary Figure a show that the Philips field lock (referred to as “Frequency Stabilization”) largely removes the gross drift but at the expense of increased field variability due to inaccuracies in determining the field rapidly from a navigator scan. Prospective frequency correction is clearly desirable, but needs to be implemented with caution.

In conclusion, MRI scans with a high gradient duty cycles, can negatively impact subsequent edited MRS acquisitions. The primary effect of frequency drift on GABA+-edited MEGA-PRESS is to cause spectral misalignment resulting in subtraction artifacts. While these errors can be remedied to some degree by post-processing frequency correction, it is best to avoid introduction of these errors, for example by ordering MR protocols such that MRS is performed before any fMRI scanning or applying prospective frequency correction.

Supplementary Material

Refer to Web version on PubMed Central for supplementary material.

Acknowledgments

This work was funded in part by NIH grants: R21 NS077300, R01 MH096263, R01 EB016089 and P41 EB015909 and DFG grant SFB 874 TP A1.

References

1. Puts NA, Edden RA. In vivo magnetic resonance spectroscopy of GABA: a methodological review. Progress in nuclear magnetic resonance spectroscopy. 2012; 60:29–41. [PubMed: 22293397]
2. Mullins PG, McGonigle DJ, O'Gorman RL, Puts NA, Vidyasagar R, Evans CJ, GABA CSoMo, Edden RAE. Current practice in the use of MEGA-PRESS spectroscopy for the detection of GABA. NeuroImage. 2012
3. Edden RA, Muthukumaraswamy SD, Freeman TC, Singh KD. Orientation discrimination performance is predicted by GABA concentration and gamma oscillation frequency in human primary visual cortex. J Neurosci. 2009; 29(50):15721–15726. [PubMed: 20016087]

4. Sumner P, Edden RA, Bompas A, Evans CJ, Singh KD. More GABA, less distraction: a neurochemical predictor of motor decision speed. Nat Neurosci. 2010; 13(7):825–827. [PubMed: 20512136]
5. Puts NA, Edden RA, Evans CJ, McGlone F, McGonigle DJ. Regionally specific human GABA concentration correlates with tactile discrimination thresholds. J Neurosci. 2011; 31(46):16556–16560. [PubMed: 22090482]
6. Boy F, Evans CJ, Edden RA, Lawrence AD, Singh KD, Husain M, Sumner P. Dorsolateral prefrontal gamma-aminobutyric acid in men predicts individual differences in rash impulsivity. Biological psychiatry. 2011; 70(9):866–872. [PubMed: 21757187]
7. Muthukumaraswamy SD, Evans CJ, Edden RA, Wise RG, Singh KD. Individual variability in the shape and amplitude of the BOLD-HRF correlates with endogenous GABAergic inhibition. Hum Brain Mapp. 2012; 33(2):455–465. [PubMed: 21416560]
8. Donahue MJ, Near J, Blicher JU, Jezzard P. Baseline GABA concentration and fMRI response. NeuroImage. 2010; 53(2):392–398. [PubMed: 20633664]
9. Muthukumaraswamy SD, Edden RA, Jones DK, Swettenham JB, Singh KD. Resting GABA concentration predicts peak gamma frequency and fMRI amplitude in response to visual stimulation in humans. Proc Natl Acad Sci U S A. 2009; 106(20):8356–8361. [PubMed: 19416820]
10. Stagg CJ. Magnetic Resonance Spectroscopy as a tool to study the role of GABA in motor-cortical plasticity. NeuroImage. 2013
11. Northoff G, Walter M, Schulte RF, Beck J, Dydak U, Henning A, Boeker H, Grimm S, Boesiger P. GABA concentrations in the human anterior cingulate cortex predict negative BOLD responses in fMRI. Nat Neurosci. 2007; 10(12):1515–1517. [PubMed: 17982452]
12. Stagg CJ, Bachtiar V, Johansen-Berg H. The role of GABA in human motor learning. Curr Biol. 2011; 21(6):480–484. [PubMed: 21376596]
13. Foerster BR, Petrou M, Edden RA, Sundgren PC, Schmidt-Wilcke T, Lowe SE, Harte SE, Clauw DJ, Harris RE. Reduced insular gamma-aminobutyric acid in fibromyalgia. Arthritis Rheum. 2012; 64(2):579–583. [PubMed: 21913179]
14. Simister RJ, McLean MA, Barker GJ, Duncan JS. Proton magnetic resonance spectroscopy of malformations of cortical development causing epilepsy. Epilepsy Res. 2007; 74(2–3):107–115. [PubMed: 17379481]
15. Maddock RJ, Buonocore MH. MR Spectroscopic Studies of the Brain in Psychiatric Disorders. Curr Top Behav Neurosci. 2012; 11:199–251.
16. Bhagwagar Z, Wylezinska M, Jezzard P, Evans J, Ashworth F, Sule A, Matthews PM, Cowen PJ. Reduction in occipital cortex gamma-aminobutyric acid concentrations in medication-free recovered unipolar depressed and bipolar subjects. Biological psychiatry. 2007; 61(6):806–812. [PubMed: 17210135]
17. Morgan PT, Pace-Schott EF, Mason GF, Forselius E, Fasula M, Valentine GW, Sanacora G. Cortical GABA levels in primary insomnia. Sleep. 2012; 35(6):807–814. [PubMed: 22654200]
18. Rojas DC, Singel D, Steinmetz S, Hepburn S, Brown MS. Decreased left perisylvian GABA concentration in children with autism and unaffected siblings. NeuroImage. 2013
19. Sanacora G, Gueorguieva R, Epperson N, Wu Y-T, Appel M, Rothman DL, Krystal JH, Mason GF. Subtype-specific alterations of ɣ-aminobutyric acid and glutamate in patients with major depression. Archives of general psychiatry. 2004; 61:705–713. [PubMed: 15237082]
20. Evans CJ, Puts NA, Robson SE, Boy F, McGonigle DJ, Sumner P, Singh KD, Edden RA. Subtraction artifacts and frequency (Mis-)alignment in J-difference GABA editing. J Magn Reson Imaging. 2012
21. Waddell KW, Avison MJ, Joers JM, Gore JC. A practical guide to robust detection of GABA in human brain by J-difference spectroscopy at 3 T using a standard volume coil. Magn Reson Imaging. 2007; 25(7):1032–1038. [PubMed: 17707165]
22. Foerster BU, Tomasi D, Caparelli EC. Magnetic field shift due to mechanical vibration in functional magnetic resonance imaging. Magn Reson Med. 2005; 54(5):1261–1267. [PubMed: 16215962]
23. Klose U. *In vivo*proton spectroscopy in presence of eddy currents. Magn Reson Med. 1990; 14(1): 26–30. [PubMed: 2161984]

24. El-Sharkawy AM, Schar M, Bottomley PA, Atalar E. Monitoring and correcting spatio-temporal variations of the MR scanner's static magnetic field. Magma. 2006; 19(5):223–236. [PubMed: 17043837]
25. Lange T, Zaitsev M, Buechert M. Correction of frequency drifts induced by gradient heating in 1H spectra using interleaved reference spectroscopy. J Magn Reson Imaging. 2011; 33(3):748–754. [PubMed: 21563261]
26. Bhattacharyya PK, Lowe MJ, Phillips MD. Spectral quality control in motion-corrupted single-voxel J-difference editing scans: an interleaved navigator approach. Magn Reson Med. 2007; 58(4):808–812. [PubMed: 17899594]
27. Gabr RE, Sathyanarayana S, Schar M, Weiss RG, Bottomley PA. On restoring motion-induced signal loss in single-voxel magnetic resonance spectra. Magn Reson Med. 2006; 56(4):754–760. [PubMed: 16964612]
28. Helms G, Piringer A. Restoration of motion-related signal loss and line-shape deterioration of proton MR spectra using the residual water as intrinsic reference. Magn Reson Med. 2001; 46(2): 395–400. [PubMed: 11477645]
29. Thiel T, Czisch M, Elbel GK, Hennig J. Phase coherent averaging in magnetic resonance spectroscopy using interleaved navigator scans: compensation of motion artifacts and magnetic field instabilities. Magn Reson Med. 2002; 47(6):1077–1082. [PubMed: 12111954]
30. Mescher M, Merkle H, Kirsch J, Garwood M, Gruetter R. Simultaneous*in vivo*spectral editing and water suppression. NMR Biomed. 1998; 11:266–272. [PubMed: 9802468]
31. Edden, RA.; Puts, NA.; Barker, PB.; Evans, CJ. Gannet: GABA analysis toolkit for edited MRS. Salt Lake City, UT: Proc ISMRM; 2013.
32. Ernst T, Kreis R, Ross BD. Absolute quantitation of water and metabolites in the human brain. I Compartments and water. J Magn Reson B. 1993; 102(1–8)
33. Helms G. Volume correction for edema in single-volume proton MR spectroscopy of contrast-enhancing multiple sclerosis lesions. Magn Reson Med. 2001; 46(2):256–263. [PubMed: 11477628]
34. Wansapura JP, Holland SK, Dunn RS, Ball WS Jr. NMR relaxation times in the human brain at 3.0 tesla. J Magn Reson Imaging. 1999; 9(4):531–538. [PubMed: 10232510]
35. Behar KL, Rothman DL, Spencer DD, Petroff OAC. Analysis of macromolecule resonances in 1H NMR spectra of human brain. Magn Reson Med. 1994; 32(3):294–302. [PubMed: 7984061]
36. Puts NA, Barker PB, Edden RA. Measuring the longitudinal relaxation time of GABA in vivo at 3 Tesla. J Magn Reson Imaging. 2013; 37(4):999–1003. [PubMed: 23001644]
37. Edden RA, Intrapiromkul J, Zhu H, Cheng Y, Barker PB. Measuring T2 in vivo with J-difference editing: application to GABA at 3 Tesla. J Magn Reson Imaging. 2012; 35(1):229–234. [PubMed: 22045601]
38. Near J, Evans CJ, Puts NA, Barker PB, Edden RA. J-difference editing of gamma-aminobutyric acid (GABA): Simulated and experimental multiplet patterns. Magn Reson Med. 2012
39. Henry P-G, Dautry C, Hantraye P, Bloch G. Brain GABA editing without macromolecule contamination. Magn Reson Med. 2001; 45:517–520. [PubMed: 11241712]
40. Near J, Simpson R, Cowen P, Jezzard P. Efficient gamma-aminobutyric acid editing at 3T without macromolecule contamination: MEGA-SPECIAL. NMR Biomed. 2011; 24(10):1277–1285. [PubMed: 21387450]
41. Edden RA, Puts NA, Barker PB. Macromolecule-suppressed GABA-edited magnetic resonance spectroscopy at 3T. Magn Reson Med. 2012; 68(3):657–661. [PubMed: 22777748]
42. Aufhaus E, Weber-Fahr W, Sack M, Tunc-Skarka N, Oberthuer G, Hoerst M, Meyer-Lindenberg A, Boettcher U, Ende G. Absence of changes in GABA concentrations with age and gender in the human anterior cingulate cortex: a MEGA-PRESS study with symmetric editing pulse frequencies for macromolecule suppression. Magn Reson Med. 2013; 69(2):317–320. [PubMed: 22488982]
43. Zhu H, Edden RA, Ouwerkerk R, Barker PB. High resolution spectroscopic imaging of GABA at 3 Tesla. Magn Reson Med. 2011; 65(3):603–609. [PubMed: 21337399]

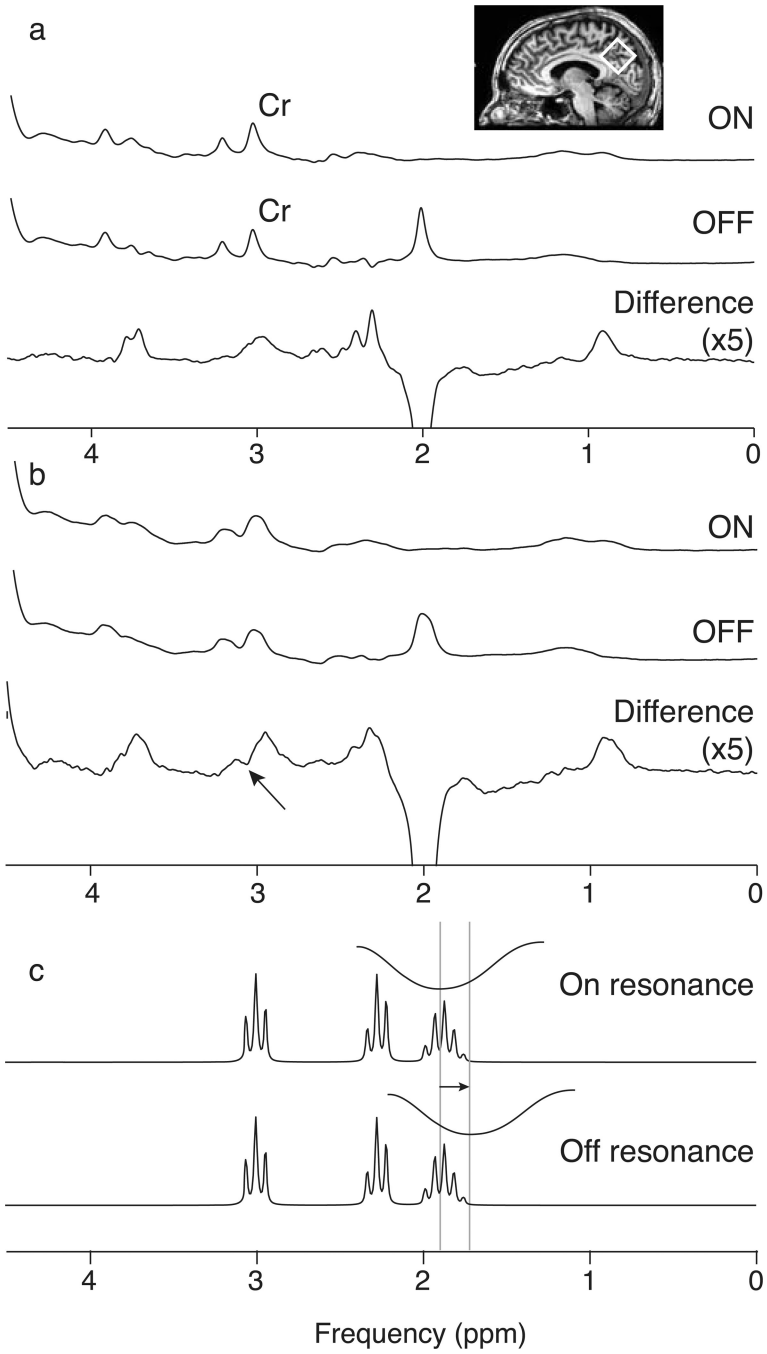

Figure 1.

Difference editing of GABA+ in the presence of B_0 field drift. (a) ON and OFF subspectra and the difference spectrum in which there is minimal frequency drift and the 3.0 ppm GABA+ peak is well resolved. Voxel placement is shown in the inset. (b) ON and OFF subspectra and the difference spectrum with frequency drift of -1.32 Hz/ min across the acquisition. Comparing (a) and (b) shows the effects of frequency drift on the linewidth of the subspectra and the introduction of a subtraction artifact (marked by an arrow) in the difference spectrum. Note that the difference spectra for both (a) and (b) are scaled by a

factor of 5 compared to the ON and OFF subspectra. (c) Schematic of the inversion envelope of the editing pulse moving 20 Hz off resonance from the 1.9 ppm GABA peak, which will reduce the efficiency of inversion at 1.9 ppm and therefore also reduce the size of the edited signal.

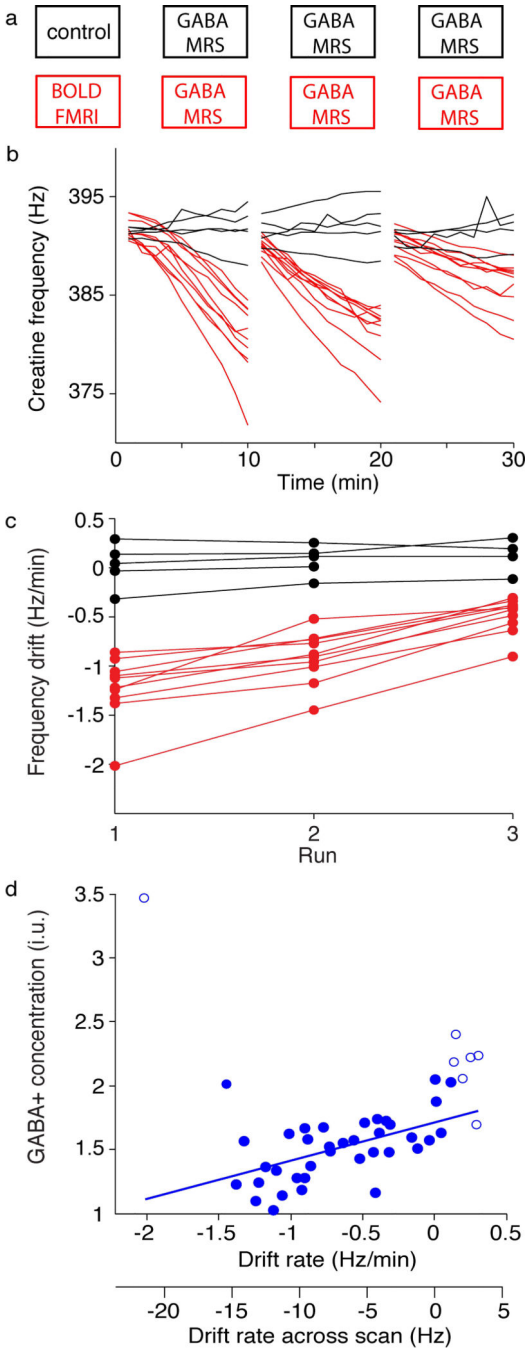

Figure 2.

Acquisition protocol and observed frequency drifts of the main *in vivo* dataset. MR protocol shown in (a): one group (shown in red) had the fMRI scan prior to the GABA-MRS acquisitions while the control group (shown in black) had only the three MRS acquisitions. (b) Frequency of the creatine peak over time during the three sequential MRS acquisitions. Red indicates acquisitions that were preceded by the 8 min fMRI acquisition and black indicates the control scans. (c) Frequency drift quantified by a linear fit of the data in (a) across each of the 3 acquisitions. (d) GABA+ concentration as a function of the frequency

drift. Open circles indicate points that were omitted in the linear fit as this data set best interrogates negative frequency drifts. The two x-axes show the frequency drift rate in units of Hz/minute as in (c), and also this rate extrapolated to total drift across the whole acquisition in units of Hz.

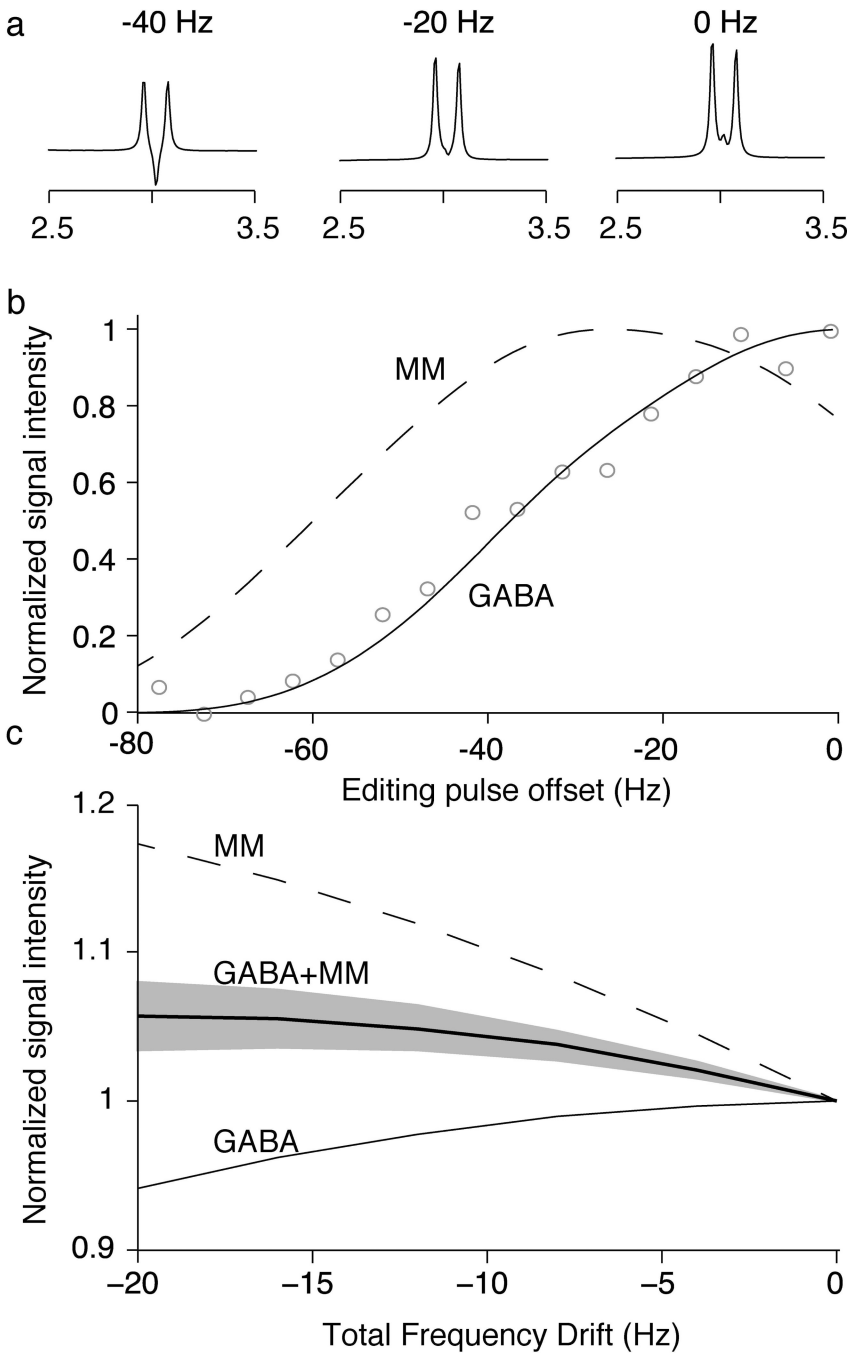

Figure 3.

Editing efficiency simulations. (a) Simulated spectra for a range of discrete editing frequency offsets. As the 1.9 ppm peak is shifted off resonance from the inversion pulse, the shape of 3.0 ppm GABA peak is altered. (b) Relative integrals of the simulated peaks for both GABA (solid line) and MM (dashed line), for a range of editing pulse offsets. GABA phantom data from a previous study (41) is shown in grey circles to demonstrate agreement between the simulations and experimental data. (c) Simulated integral of the 3.0 ppm GABA peak (solid line) and the MM peak (dashed line) as a function of frequency drift occurring

throughout the experiment, normalized to the signals at 0 Hz offset. The net impact of frequency drift on the GABA and MM peaks for quantified GABA+ is shown as a thick line assuming 50:50 signal contributions for GABA and MM and as a shaded area for the range of 40:60 to 60:40 signal contributions for GABA and MM at zero drift.

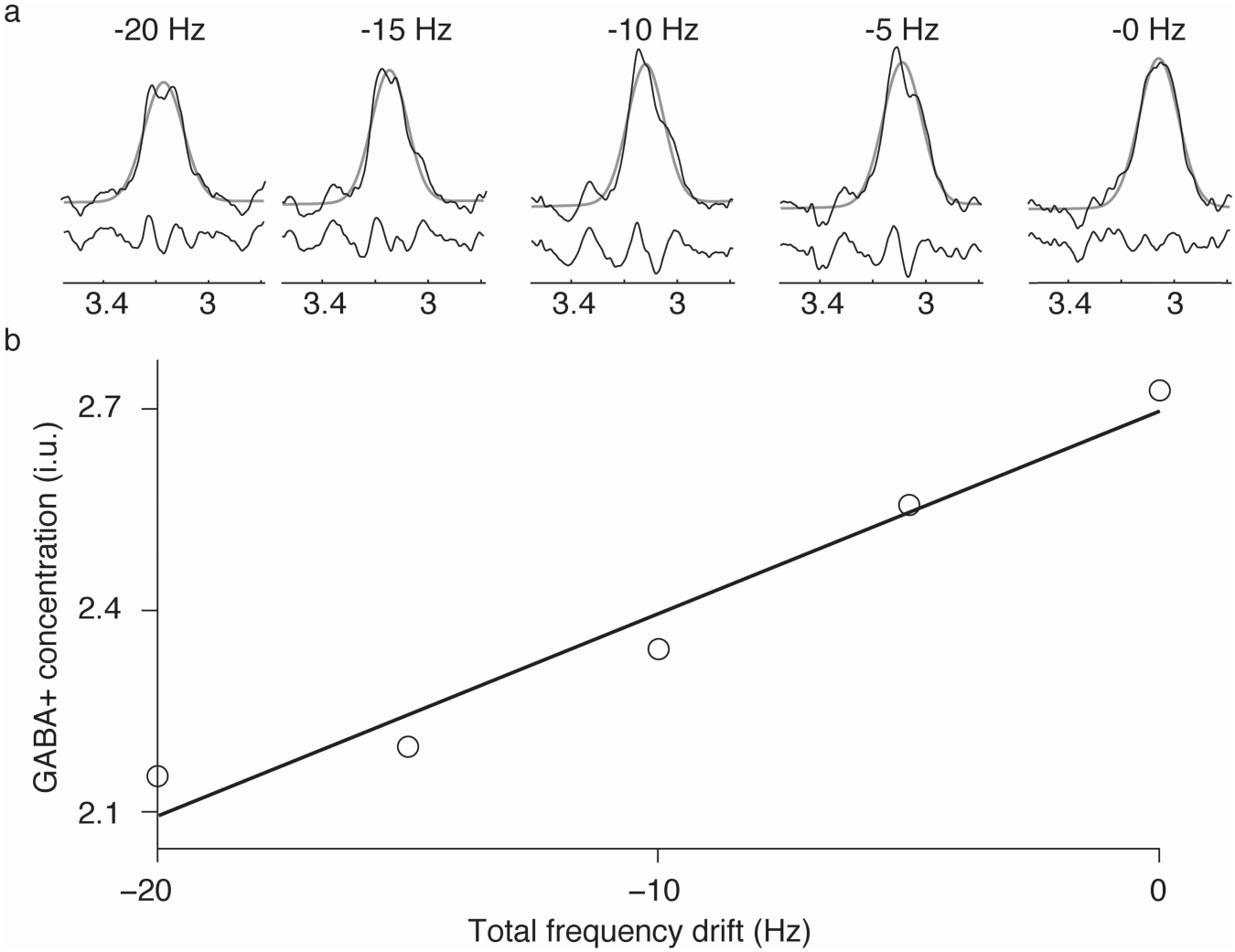

Figure 4.

Frequency drifts of -5 to -20 Hz applied to previously well-aligned data to examine subtraction artifacts. (a) The difference spectrum (in black) and the Gaussian fit (in gray) with the residuals below for total drifts of -20 Hz, -15 Hz, -10 Hz, -5 Hz and no drift across the acquisition. (b) Quantified GABA+ as a function of the total amount of frequency drift.

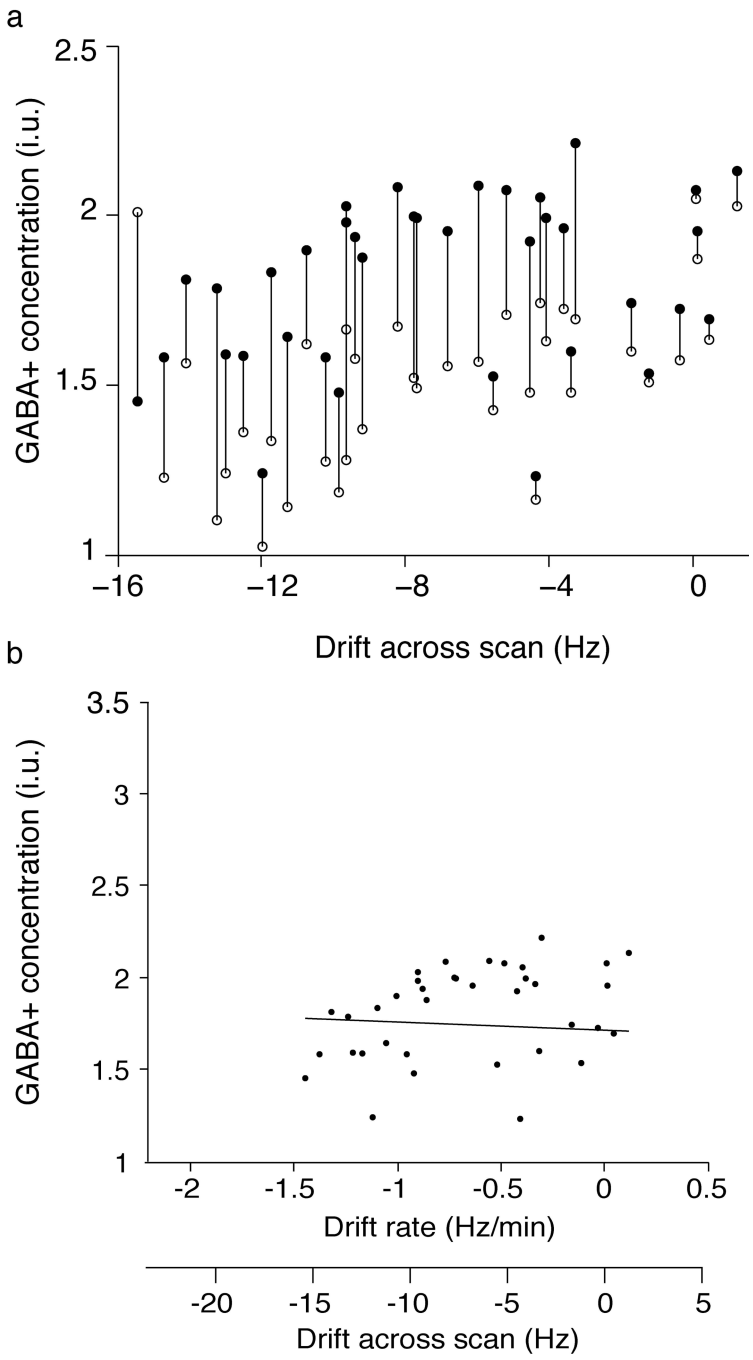

Figure 5.

Changes in measured GABA+ concentration as a result of post-processing frequency correction. (a) Measured GABA+ concentration for each MRS acquisition before (open circles) and after frequency correction (closed circles). (b) Frequency-corrected estimates of GABA+ concentration as a function of frequency drift. The linear fit of this data has a slope of 0.0071 i.u./Hz indicating that the apparent linear dependency between GABA+ concentration and frequency drift is essentially removed after frequency correction.